

# Relationship between Progressive Changes in Lamina Cribrosa Depth and Deterioration of Visual Field Loss in Glaucomatous Eyes

You Na Kim<sup>1</sup>, Joong Won Shin<sup>2</sup>, Kyung Rim Sung<sup>1</sup>

<sup>1</sup>Department of Ophthalmology, Asan Medical Center, University of Ulsan College of Medicine, Seoul, Korea

<sup>2</sup>Department of Ophthalmology, Gangneung Asan Hospital, University of Ulsan College of Medicine, Gangneung, Korea

**Purpose:** To investigate the relationship between the progression of visual field (VF) loss and changes in lamina cribrosa depth (LCD) as determined by spectral-domain optical coherence tomography (SD-OCT) enhanced depth imaging in patients with primary open angle glaucoma (POAG).

**Methods:** Data from 60 POAG patients (mean follow-up,  $3.5 \pm 0.7$  years) were included in this retrospective study. The LCD was measured in the optic disc image using SD-OCT enhanced depth imaging scanning at each visit. Change in the LCD was considered to either 'increase' or 'decrease' when the differences between baseline and the latest two consecutive follow-up visits were greater than the corresponding reproducibility coefficient value ( $23.08 \mu\text{m}$ , as determined in a preliminary reproducibility study). All participants were divided into three groups: increased LCD (ILCD), decreased LCD (DLCD), and no LCD change (NLCD). The Early Manifest Glaucoma Trial criteria were used to define VF deterioration. Kaplan-Meier survival analysis and Cox's proportional hazard models were performed to explore the relationship between VF progression and LCD change.

**Results:** Of the 60 eyes examined, 35.0% (21 eyes), 28.3% (17 eyes), and 36.7% (22 eyes) were classified as the ILCD, DLCD, and NLCD groups, respectively. Kaplan-Meier survival analysis showed a greater cumulative probability of VF progression in the ILCD group than in the NLCD ( $p < 0.001$ ) or DLCD groups ( $p = 0.018$ ). Increased LCD was identified as the only risk factor for VF progression in the Cox proportional hazard models (hazard ratio, 1.008; 95% confidence interval, 1.000 to 1.015;  $p = 0.047$ ).

**Conclusions:** Increased LCD was associated with a greater possibility of VF progression. The quantitative measurement of LCD changes, determined by SD-OCT, is a potential biomarker for the prediction of VF deterioration in patients with POAG.

**Key Words:** Glaucoma, Lamina cribrosa, Optic disk, Optical coherence tomography, Visual fields

Glaucoma is a leading cause of irreversible blindness and is thought to arise primarily as a result of structural changes

in the lamina cribrosa (LC) of the optic nerve head (ONH) [1-3]. With the advent of optical coherence tomography (OCT), numerous studies have been performed to characterize the structure of the LC in glaucomatous eyes [4-6]. In comparison with normal eyes, the LC was thinner in glaucomatous eyes [7] and was also found to be posteriorly displaced, which is accompanied by enlargement of the optic disc cup, as observed on stereoscopic examination

Received: January 29, 2018 Accepted: April 2, 2018

Corresponding Author: Kyung Rim Sung, MD, PhD. Department of Ophthalmology, Asan Medical Center, University of Ulsan College of Medicine, #88 Olympic-ro 43-gil, Songpa-gu, Seoul 05505, Korea. Tel: 82-2-3010-3680, Fax: 82-2-470-6440, E-mail: sungeye@gmail.com

© 2018 The Korean Ophthalmological Society

This is an Open Access article distributed under the terms of the Creative Commons Attribution Non-Commercial License (<http://creativecommons.org/licenses/by-nc/3.0/>) which permits unrestricted non-commercial use, distribution, and reproduction in any medium, provided the original work is properly cited.

of the ONH [8-10].

Previous studies show posterior displacement of the LC to occur prior to the development of retinal nerve fiber layer (RNFL) defects in the glaucomatous ONH [11] and show the degree of posterior displacement to be greater in eyes with visual field (VF) defects than in eyes without VF defects [10]. While a relationship between greater LC depth (LCD) and a faster rate of RNFL thinning has been reported in patients with glaucoma [12-14], several other studies find no relationship between LCD and glaucomatous functional status [15]. As glaucomatous structural change precedes functional deficit, these results suggest that posterior displacement of the LC may occur in the early stages; as the disease progresses, VF deterioration progresses further even though the LC may remain in the same position. On the basis of these data, we hypothesize that the posterior movement of the LC may be a predictor of subsequent VF progression. In this study, we explored the longitudinal changes in LCD in glaucomatous eyes by reviewing serial images obtained from spectral domain (SD)-OCT enhanced depth imaging (EDI) scanning. In addition, we explored the factors associated with VF progression in glaucomatous eyes, including LCD change.

## Materials and Methods

### Subjects

The data were collected from an ongoing basis with 6-month interval. We performed a retrospective review of the medical records of all subjects who had attended the glaucoma clinic at the Asan Medical Center, Seoul, Republic of Korea from March, 2011 to June, 2016. At the first visit, all subjects underwent a comprehensive ophthalmologic examination including a review of medical and ophthalmic history, measurement of best-corrected visual acuity, slit-lamp biomicroscopy, Goldmann applanation tonometry, gonioscopy, central corneal thickness assessment (DGH-550 instrument; DGH Technology, Exton, PA, USA), funduscopy examination, axial length (IOLMaster; Carl Zeiss Meditec, Dublin, CA, USA), stereoscopic optic disc photography, red-free photography, standard automated perimetry (Humphrey Field analyzer [HFA] with Swedish Interactive Threshold Algorithm standard 24-2 test, Carl Zeiss Meditec), and ONH imaging with a SD-OCT (Heidel-

berg Engineering, Dossenheim, Germany). For study inclusion, participants were required to have a best-corrected visual acuity 20 / 40 or better and normal anterior chamber and open-angle on slit-lamp and gonioscopic examinations. Glaucoma patients were identified by the presence of RNFL defects on red-free photography or the presence of glaucomatous optic disc changes on optic disc photography (such as enlarged cup-to-disc ratio [ $>0.7$ ], diffuse or focal neural rim thinning, or disc hemorrhage) and the presence of VF defects that corresponded with RNFL defects and optic disc changes. All subjects were followed up at 6-month intervals with stereoscopic optic disc photography, red-free photography, VF testing, and ONH imaging with SD-OCT. All tests were performed at the same visit or within 2 weeks; individuals had  $\geq 2$  years follow-up, with at least four qualified images obtained at different visits. All accepted images exhibited a centered optic disc, were well focused, and had even and adequate illumination. Subjects with any ophthalmic or neurologic disease known to affect ONH or VF were excluded. Patients who underwent intraocular surgical treatment during follow-up but had  $>2$  years follow-up prior to surgery, were included in the study (only data obtained prior to surgery were analyzed). The study was approved by the institutional review board of the Asan Medical Center (2014-0311), and the study design conformed to the Declaration of Helsinki. Informed consent was waived due to the retrospective nature of the study.

### Assessment of LC change by SD-OCT

The ONH was examined using SD-OCT EDI scanning at each visit. Two experienced observers (YNK and JWS) manually measured the LCD within the ONH using ImageJ software ver. 1.48 (National Institutes of Health, Bethesda, MD, USA; <http://imagej.nih.gov/ij>). Briefly, the entire optic disc was scanned using a 6-mm line (512 A-scans) with an interval of 50  $\mu\text{m}$ . In our study, an average of 35 horizontal B-scans was produced in EDI mode. From these B-scans, five frames (center, mid-superior, superior, mid-inferior, and inferior) that passed through the optic disc were selected. The structure of the optic disc was analyzed with the intrinsic viewer. The Bruch's membrane opening (BMO; two red points in Fig. 1A, 1B) was defined by the proximal tips of the Bruch's membrane and a line connecting the BMO on each side was regarded as the BMO plane. The anterior LC surface was set as the hori-

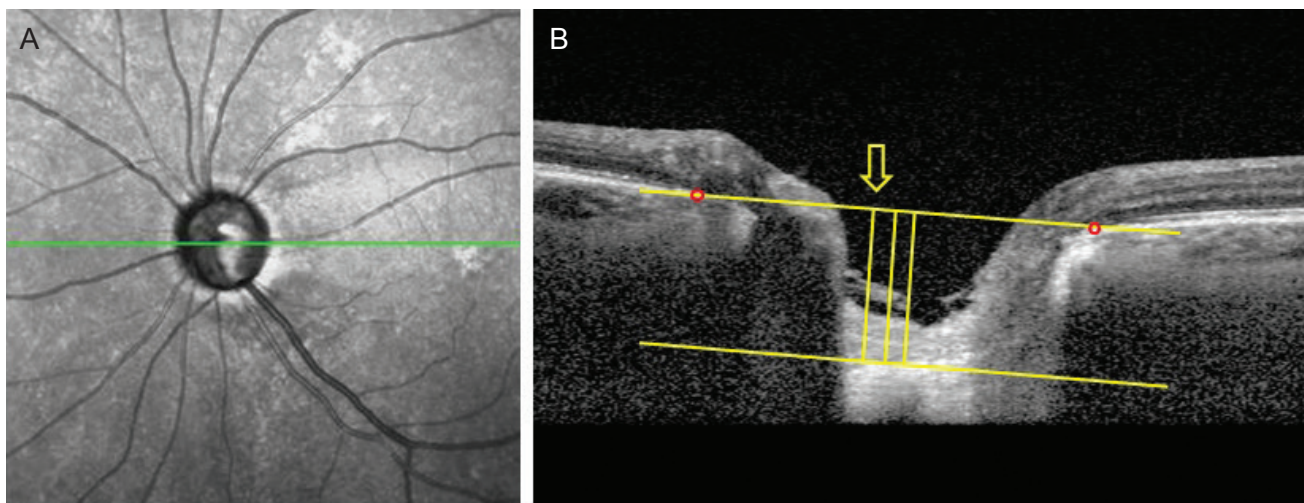


**Fig. 1.** Measurement of lamina cribrosa depth (LCD) by spectral-domain optical coherence tomography. (A) En-face images of the optic nerve head were obtained from spectral-domain optical coherence tomography enhanced depth imaging scanning. Among several B-scans from optic disc scanning, a horizontal section image passing through major vessel trunks was selected to measure the LCD. This image-selecting procedure was repeated in the same eye at each follow up visit. (B) A line connecting the Bruch's membrane opening (red dots) on each side was regarded as the Bruch's membrane opening plane. The anterior surface of the lamina cribrosa was set as the horizontal margin, where the highly reflective region beneath the optic disc cup started. The distance of the three perpendicular lines (composed of the maximally depressed point, yellow arrow) from the reference line, and 100 and 200  $\mu\text{m}$  apart from the maximally depressed point to temporal direction, were measured. A manual caliper tool and regions of interest manager of ImageJ software was used for each measurement and the LCD was determined by the average value measured from the three points.

zontal margin where the highly reflective region beneath the optic disc cup started. The maximum perpendicular depth from the BMO plane to the anterior LC surface was measured. The depths were measured from two additional points 100 and 200  $\mu\text{m}$  from the maximum distance point to the temporal direction. The average of three depths was defined as the LCD of each frame. Since the nasal part of the anterior LC surface was usually indistinguishable due to the shadow of the central vessel trunk, only temporally adjacent points were considered. The LCD of each eye was determined by averaging the LCD values from the 5 selected frames at each visit. The mean of the two values obtained from each examiner was used in the main analysis. Details of the measurement have been described previously [16]. Before the main analysis, inter-examiner and intra-class correlation coefficients were calculated using 25 randomly selected images to test reproducibility.

A statistically significant change in LCD was determined by event-based analysis and the criterion for meaningful change was distinguished by the value of the reproducibility coefficient (RC). The RC value was considered as the value under which the difference between any two repeat measurements on the same subject fell with 95% probability, and was calculated as  $1.96 \times \sqrt{2} \times$  (standard deviation of

LCD change), 23.08  $\mu\text{m}$  [17]. Comparing the LCDs between the baseline and latest two consecutive visits, the subjects were classified into three groups. Eyes with an increase of LCD  $>23.08 \mu\text{m}$  or decrease of LCD  $<-23.08 \mu\text{m}$  were classified as the increased LCD (ILCD) group or decreased LCD (DLCD) group, respectively. The remaining eyes were classified as the no LCD change (NLCD) group. Representative examples are shown in Fig. 2A-2C.

#### Analysis of VF progression in glaucomatous eyes

Standard automated perimetry was performed with a HFA Swedish Interactive Threshold Algorithm standard 24-2 test at each follow-up visit at least 6 months apart. Using these data, the Early Manifest Glaucoma Trial criteria were used to define VF progression during follow-up [18]. The rate of visual field index reduction, determined by a negative linear slope from guided progression analysis in the HFA, was also estimated.

#### Statistical analysis

The Shapiro-Wilk test was performed to confirm the normality of the variables. Since none of them were veri-

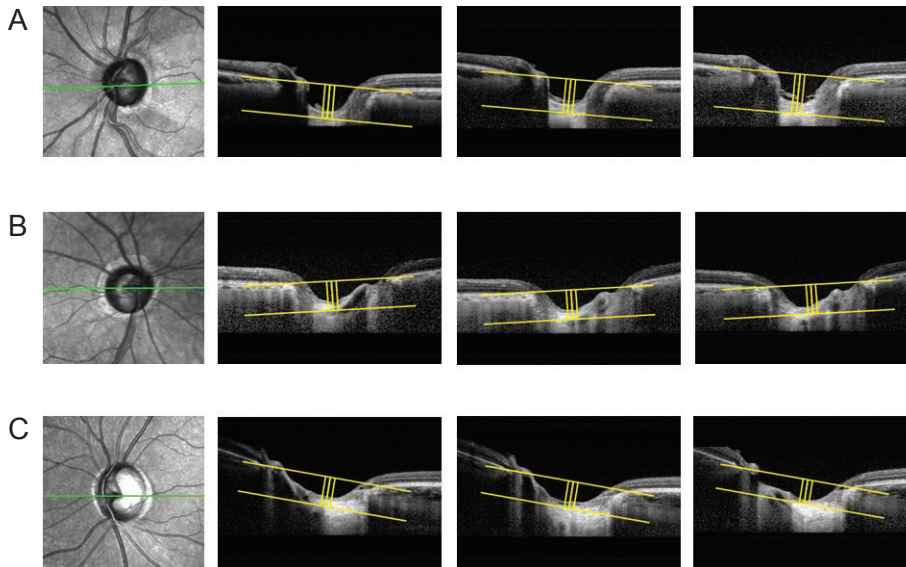


**Fig. 2.** Subgroup analysis of lamina cribrosa displacement. The method of measuring lamina cribrosa depth (LCD) described in Fig. 1 was repeated at each follow-up visit. The values were determined at each follow-up visit and the difference from the first to the last measurement was considered LCD change. A significant LCD change was defined as a value greater, within and less than the reproducibility coefficient ( $23.08 \mu\text{m}$ ). (A) Posteriorly displaced lamina cribrosa (LC), (B) no significant LC displacement, and (C) anteriorly displaced LC.

fied to be significant, the normal distribution of the variables was assumed. Baseline characteristics were subsequently compared among the three groups using ANOVA (post hoc analysis, Tukey's test). Kaplan-Meier survival analyses were conducted to explore and compare the cumulative probability of VF progression among the three groups (log-rank test). The hazard ratios (HRs) of clinical factors for VF progression were evaluated using univariate and multivariate Cox proportional hazard models with the time point of VF progression defined by Early Manifest Glaucoma Trial as a time-dependent covariate. Univariate analyses were performed separately for each variable and factors with a  $p$ -value  $<0.20$  were included in multivariate analysis with a 'forward: conditional method' to calculate the HRs and 95% confidence intervals (CIs) to identify the influential variables for VF progression. All statistical analyses were performed with IBM SPSS ver. 22 (IBM Corp., Armonk, NY, USA) and a  $p$ -value  $<0.05$  was considered statistically significant.

## Results

Of the 69 eyes that met the other inclusion criteria, nine were excluded due to poor SD-OCT image quality. Therefore, 60 eyes from 60 primary open angle glaucoma patients (27 male and 33 female) were included in this study; the mean follow-up duration was  $3.5 \pm 0.7$  years. Baseline characteristics are summarized in Table 1. Excellent in-

ter-observer reproducibility was observed (intraclass correlation coefficient =  $0.991$  [ $0.986$ – $0.995$ ],  $p < 0.001$ ).

The assessed eyes were classified into three groups: ILCD ( $n = 21$ , 35.0%), NLCD ( $n = 22$ , 36.7%), and DLCD ( $n = 17$ , 28.3%). Typical images from each group are illustrated in Fig. 2. With the exception of LCD change, there were no significant differences between the three groups in terms of baseline variables such as axial length, central corneal thickness, intraocular pressure (IOP) reduction rate during follow up period, and rate of visual field index change (Table 1).

To compare the cumulative probability of VF progression between the three groups, Kaplan-Meier survival analyses were conducted (Fig. 3). The ILCD group showed a greater cumulative probability of VF progression during the follow-up period than the NLCD ( $p < 0.001$ ) and DLCD groups ( $p = 0.018$ ).

Univariate analysis of Cox's proportional hazard models was used to assess the association between potential risk factors and VF progression (Table 2). Among the baseline parameters, axial length (HR, 1.249; 95% CI, 0.954 to 1.634;  $p = 0.106$ ), follow-up IOP (HR, 1.226; 95% CI, 0.985 to 1.525;  $p = 0.068$ ), and the change in LCD (HR, 1.008; 95% CI, 1.000 to 1.016;  $p = 0.049$ ) showed a possible association with VF progression ( $p < 0.2$ ). Using these selected variables, multivariate analysis was performed to identify factors associated with VF progression; change of LCD was the only statistically significant variable (HR, 1.008; 95% CI, 1.000 to 1.015;  $p = 0.047$ ).

**Table 1.** Comparison of baseline characteristics among the study groups

Parameter	All subjects	ILCD	NLCD	DLCD	p-value*
Eyes	60	21	22	17	
Age (yr)	49.73 ± 13.53	48.67 ± 13.25	51.95 ± 13.25	48.18 ± 14.64	0.630
Ocular factor					
Axial length (mm)	25.22 ± 1.77	25.25 ± 1.82	25.02 ± 1.64	25.43 ± 1.95	0.773
CCT (µm)	532.34 ± 32.28	529.60 ± 37.22	531.98 ± 30.32	536.20 ± 29.65	0.825
Baseline IOP (mmHg)	15.92 ± 3.38	15.43 ± 2.82	15.73 ± 4.01	16.76 ± 3.15	0.452
Follow up IOP (mmHg)	14.33 ± 2.25	14.67 ± 2.08	14.36 ± 2.61	13.88 ± 2.00	0.572
IOP reduction (%) <sup>†</sup>	6.91 ± 20.80	2.18 ± 20.94	5.06 ± 22.28	15.16 ± 17.05	0.140
Perimetric parameter					
Baseline MD (dB)	-6.94 ± 4.53	-7.53 ± 4.77	-5.53 ± 4.46	-8.03 ± 4.06	0.177
Rate of VFI change (%)	-0.63 ± 1.43	-0.94 ± 1.87	-0.29 ± 1.15	-0.68 ± 1.04	0.322
Optic disc parameter					
Baseline LCD (µm)	558.15 ± 145.41	562.80 ± 142.36	534.04 ± 159.99	583.62 ± 132.37	0.566
LCD change (µm)	-2.13 ± 63.87	58.56 ± 36.27	-1.17 ± 14.31	-78.42 ± 45.81	<0.001*
					<0.001 <sup>‡</sup> <0.001 <sup>§</sup> <0.001 <sup>¶</sup>

Values are presented as number or mean ± standard deviation.

LCD = lamina cribrosa depth; ILCD = increased LCD; NLCD = no LCD change; DLCD = decreased LCD; CCT = central corneal thickness; IOP = intraocular pressure; MD = mean deviation; VFI = visual field index.

\*p < 0.05 considered as statistically significant; <sup>†</sup>IOP reduction = (baseline IOP - follow up IOP) / baseline IOP × 100. Intergroup ANOVA testing was performed using the mean values. If p-values were <0.05, post hoc analysis (Tukey's test) was performed; <sup>‡</sup>p-value for the post hoc analysis of the ILCD and NLCD groups; <sup>§</sup>p-value for the post hoc analysis of the NLCD and DLCD groups; <sup>¶</sup>p-value for the post hoc analysis of the ILCD and DLCD groups.

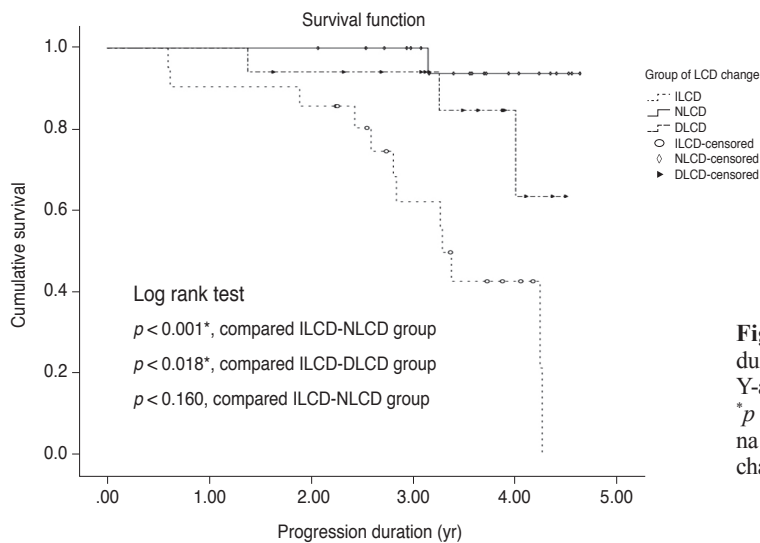


**Fig. 3.** Kaplan-Meier estimates of visual field progression during the follow up period. X-axis, follow-up period (year); Y-axis, cumulative probability of the visual field progression. \*p < 0.05 considered as statistically significant. LCD = lamina cribrosa depth; ILCD = increased LCD; NLCD = no LCD change; DLCD = decreased LCD.

## Discussion

Posterior displacement of the LC in glaucoma has been described in a range of investigations, including animal models [2,9] and human studies [10,19,20]. Inspired by

these previous studies, our retrospective clinical study was designed to determine whether posterior movement of the LC could be a predictor of VF progression in glaucomatous eyes.

In patients with primary open angle glaucoma, we found

**Table 2.** Univariate and multivariate Cox's proportional hazard models for prediction of visual field progression

Parameter	Univariate analysis		Univariate analysis	
	HR (95% CI)	<i>p</i> -value	HR (95% CI)	<i>p</i> -value
Age (yr)	0.991 (0.957–1.026)	0.597		
Ocular factor				
Axial length (mm)	1.249 (0.954–1.634)	0.106 <sup>†</sup>	1.301 (0.983–1.721)	0.066
CCT (μm)	1.007 (0.990–1.024)	0.418		
Baseline IOP (mmHg)	1.020 (0.881–1.181)	0.791		
Follow up IOP (mmHg)	1.226 (0.985–1.525)	0.068 <sup>†</sup>	1.215 (0.974–1.516)	0.084
IOP reduction (%) <sup>*</sup>	0.993 (0.972–1.013)	0.482		
Perimetric parameter				
Baseline MD (dB)	0.970 (0.874–1.077)	0.571		
Optic disc parameter				
Baseline LCD (μm)	1.001 (0.998–1.004)	0.432		
LCD change (μm)	1.008 (1.000–1.016)	0.050 <sup>†</sup>	1.008 (1.000–1.015)	0.047 <sup>†</sup>

HR = hazard ratio; CI = confidence interval; CCT = central corneal thickness; IOP = intraocular pressure; MD = mean deviation; LCD = lamina cribrosa depth.

<sup>\*</sup>Univariate factors under  $p < 0.2$  were re-evaluated multivariate Cox analysis; <sup>†</sup> $p < 0.05$  considered as statistically significant.

that the LC moved posteriorly (ILCD group) in 21 eyes examined (35.0%) and anteriorly (DLCD group) in 17 eyes (28.3%) during the follow-up period. The RC value of 23.08 μm was used as a reference value for the classification of the three groups according to the change in LCDs and this value has a similar range of repeatability estimate from that of a previous study [21]. Among the three groups, other than change in LCD, there were no statistically significant differences in investigated parameters, including axial length, IOP and baseline LCD. However, the ILCD group showed a significantly greater probability of VF progression than either the NLCD or the DLCD groups during follow-up when assessed by the Kaplan-Meier survival test.

The observed association between ILCD and VF progression can be explained by the association between deformation of the LC and VF progression, as demonstrated in a previous study [22]. The LC is a sieve-like connective tissue structure through which retinal ganglion cell axons pass as they exit the eye. As it is thought to be the principal site of retinal ganglion cell axonal injury [23,24], posterior LC displacement may impose further compression, extension, and shear stress on the axons passing through the laminar pores resulting in the loss of neuronal function of the axons as well as damage to the capillaries present in the LC [25]. An additional study demonstrated that the region of LC deformation showed good spatial correlation between RNFL loss

and VF defect, compared with normal eyes [10,19]. Therefore, the posterior movement of the LC observed in this study represents an early biomarker of VF progression in glaucomatous eyes.

Interestingly, a substantial portion of eyes showed anterior movement of the LC (28.3%). Although the probability of VF progression was less than that seen in the ILCD group, the DLCD group also showed VF progression to a greater extent than the NLCD group. As glaucoma patients in this study received IOP-lowering treatment during the follow-up period, the anterior LC movement can be considered to occur as a consequence of IOP reduction and be related to scleral expansion, as shown in previous studies [15,26-28]. Therefore, VF progression in this group can be interpreted as a progressive worsening of glaucoma despite control of IOP and reduction of LC depth.

Our study has several limitations. When reviewing SD-OCT EDI scanning data retrospectively, we had to exclude 13% of the subjects because image quality was insufficient to identify the deep anatomical structure of the LC. A prospective study is required to optimize the scanning protocol in order to increase the resolution of OCT images. Secondly, there may be a bias in the process of measuring LCD with BMO as a reference plane. Because the choroid lies between the sclera and Bruch's membrane, changes in choroidal thickness due to aging, axial length, or diurnal variations

could influence the measured LCD [29,30]. Future study is needed to measure LCD with anterior scleral canal opening as a reference plane, which would exclude choroidal thickness [21]. Thirdly, our study is limited in obtaining only five B-scan frames to measure the LCDs and this may not represent all features of the LCD. Finally, due to the small sample size, subgroup analysis according to the level of glaucoma severity was not conducted. Further investigation will be required to determine the relationship between LC movement and VF progression in patients with pre-perimetric or early and advanced stage glaucoma, as the relationship can be different according to the level of glaucoma severity.

Despite the limitations described above, we believe that our study has strength because we investigated long-term progressive change of LCD compared with previous studies that measured LCD cross-sectionally or for a relatively short-term period [10,21]. In conclusion, the assessment of LCD change can be a useful biomarker to predict future VF progression in glaucoma patients. In particular, posterior movement of the LC was associated with a higher risk of subsequent VF progression.

## Conflict of Interest

No potential conflict of interest relevant to this article was reported.

## References

1. Quigley HA, Addicks EM, Green WR, Maumenee AE. Optic nerve damage in human glaucoma. II. The site of injury and susceptibility to damage. *Arch Ophthalmol* 1981;99:635-49.
2. Quigley HA, Anderson DR. Distribution of axonal transport blockade by acute intraocular pressure elevation in the primate optic nerve head. *Invest Ophthalmol Vis Sci* 1977;16:640-4.
3. Radius RL, Anderson DR. Rapid axonal transport in primate optic nerve. Distribution of pressure-induced interruption. *Arch Ophthalmol* 1981;99:650-4.
4. Kim TW, Kagemann L, Girard MJ, et al. Imaging of the lamina cribrosa in glaucoma: perspectives of pathogenesis and clinical applications. *Curr Eye Res* 2013;38:903-9.
5. Nadler Z, Wang B, Wollstein G, et al. Repeatability of in vivo 3D lamina cribrosa microarchitecture using adaptive optics spectral domain optical coherence tomography. *Biomed Opt Express* 2014;5:1114-23.
6. Vilupuru AS, Rangaswamy NV, Frishman LJ, et al. Adaptive optics scanning laser ophthalmoscopy for in vivo imaging of lamina cribrosa. *J Opt Soc Am A Opt Image Sci Vis* 2007;24:1417-25.
7. Chung HS, Sung KR, Lee KS, et al. Relationship between the lamina cribrosa, outer retina, and choroidal thickness as assessed using spectral domain optical coherence tomography. *Korean J Ophthalmol* 2014;28:234-40.
8. Burgoyne CF, Downs JC. Premise and prediction-how optic nerve head biomechanics underlies the susceptibility and clinical behavior of the aged optic nerve head. *J Glaucoma* 2008;17:318-28.
9. Yang H, Downs JC, Bellezza A, et al. 3-D histomorphometry of the normal and early glaucomatous monkey optic nerve head: prelaminar neural tissues and cupping. *Invest Ophthalmol Vis Sci* 2007;48:5068-84.
10. Furlanetto RL, Park SC, Damle UJ, et al. Posterior displacement of the lamina cribrosa in glaucoma: in vivo interindividual and intereye comparisons. *Invest Ophthalmol Vis Sci* 2013;54:4836-42.
11. Xu G, Weinreb RN, Leung CK. Optic nerve head deformation in glaucoma: the temporal relationship between optic nerve head surface depression and retinal nerve fiber layer thinning. *Ophthalmology* 2014;121:2362-70.
12. Lee EJ, Kim TW, Kim M, Kim H. Influence of lamina cribrosa thickness and depth on the rate of progressive retinal nerve fiber layer thinning. *Ophthalmology* 2015;122:721-9.
13. Omodaka K, Takahashi S, Matsumoto A, et al. Clinical factors associated with lamina cribrosa thickness in patients with glaucoma, as measured with swept source optical coherence tomography. *PLoS One* 2016;11:e0153707.
14. Chung HS, Sung KR, Lee JY, Na JH. Lamina cribrosa-related parameters assessed by optical coherence tomography for prediction of future glaucoma progression. *Curr Eye Res* 2016;41:806-13.
15. Lee EJ, Kim TW, Weinreb RN. Reversal of lamina cribrosa displacement and thickness after trabeculectomy in glaucoma. *Ophthalmology* 2012;119:1359-66.
16. Kim S, Sung KR, Lee JR, Lee KS. Evaluation of lamina cribrosa in pseudoexfoliation syndrome using spectral-domain optical coherence tomography enhanced depth imaging. *Ophthalmology* 2013;120:1798-803.

17. Vaz S, Falkmer T, Passmore AE, et al. The case for using the repeatability coefficient when calculating test-retest reliability. *PLoS One* 2013;8:e73990.
18. Heijl A, Leske MC, Bengtsson B, et al. Measuring visual field progression in the Early Manifest Glaucoma Trial. *Acta Ophthalmol Scand* 2003;81:286-93.
19. Lee EJ, Kim TW, Weinreb RN, et al. Three-dimensional evaluation of the lamina cribrosa using spectral-domain optical coherence tomography in glaucoma. *Invest Ophthalmol Vis Sci* 2012;53:198-204.
20. Bellezza AJ, Rintalan CJ, Thompson HW, et al. Anterior scleral canal geometry in pressurised (IOP 10) and non-pressurised (IOP 0) normal monkey eyes. *Br J Ophthalmol* 2003;87:1284-90.
21. Vianna JR, Lanoe VR, Quach J, et al. Serial changes in lamina cribrosa depth and neuroretinal parameters in glaucoma: impact of choroidal thickness. *Ophthalmology* 2017;124:1392-402.
22. Faridi OS, Park SC, Kabadi R, et al. Effect of focal lamina cribrosa defect on glaucomatous visual field progression. *Ophthalmology* 2014;121:1524-30.
23. Minckler DS, Bunt AH, Johanson GW. Orthograde and retrograde axoplasmic transport during acute ocular hypertension in the monkey. *Invest Ophthalmol Vis Sci* 1977;16:426-41.
24. Quigley HA, Addicks EM. Regional differences in the structure of the lamina cribrosa and their relation to glaucomatous optic nerve damage. *Arch Ophthalmol* 1981;99:137-43.
25. Sigal IA, Flanagan JG, Tertinegg I, Ethier CR. Predicted extension, compression and shearing of optic nerve head tissues. *Exp Eye Res* 2007;85:312-22.
26. Reis AS, O'Leary N, Stanfield MJ, et al. Lamellar displacement and prelaminar tissue thickness change after glaucoma surgery imaged with optical coherence tomography. *Invest Ophthalmol Vis Sci* 2012;53:5819-26.
27. Lee EJ, Kim TW, Weinreb RN, Kim H. Reversal of lamina cribrosa displacement after intraocular pressure reduction in open-angle glaucoma. *Ophthalmology* 2013;120:553-9.
28. Sigal IA, Yang H, Roberts MD, et al. IOP-induced lamina cribrosa displacement and scleral canal expansion: an analysis of factor interactions using parameterized eye-specific models. *Invest Ophthalmol Vis Sci* 2011;52:1896-907.
29. Chakraborty R, Read SA, Collins MJ. Diurnal variations in axial length, choroidal thickness, intraocular pressure, and ocular biometrics. *Invest Ophthalmol Vis Sci* 2011;52:5121-9.
30. Rho CR, Park HY, Lee NY, Park CK. Clock-hour lamellar displacement and age in primary open-angle glaucoma and normal tension glaucoma. *Clin Exp Ophthalmol* 2012;40:e183-9.